Open

Oncogene (2012) 31, 3635–3646

www.nature.com/onc

ORIGINAL ARTICLE

Igf2 ligand dependency of *Pten*$^{+/-}$ developmental and tumour phenotypes in the mouse

DN Church[1], BR Phillips[2], DJ Stuckey[3,5], DJ Barnes[1], FM Buffa[4], S Manek[2], K Clarke[3], AL Harris[4], EJ Carter[1] and AB Hassan[1]

[1]*Sir William Dunn School of Pathology, University of Oxford, Oxford, UK;* [2]*Department of Histopathology, John Radcliffe Hospital, Headington, Oxford, UK;* [3]*Department of Physiology, Anatomy and Genetics, University of Oxford, Oxford, UK and* [4]*Weatherall Institute of Molecular Medicine, University of Oxford, John Radcliffe Hospital, Headington, Oxford, UK*

The tumour suppressor PTEN is a key negative regulator of the PI3K-Akt pathway, and is frequently either reduced or lost in human tumours. Murine genetic studies have confirmed that reduction of Pten promotes tumourigenesis in multiple organs, and demonstrated dependency of tumour development on the activation of downstream components such as Akt. Insulin-like growth factors (IGFs) act via IGF1R to activate the PI3K-Akt pathway, and are commonly upregulated in cancer. A context-dependent interplay between IGFs and PTEN exists in normal tissue and tumours; increased IGF2 ligand supply induces Pten expression creating an autoregulatory negative feedback loop, whereas complete loss of PTEN may either cooperate with IGF overexpression in tumour promotion, or result in desensitisation to IGF ligand. However, it remains unknown whether neoplasia associated with Pten loss is dependent on upstream IGF ligand supply *in vivo*. We evaluated this by generation of *Pten*$^{+/-}$ mice with differing allelic dosage of *Igf2*, an imprinted gene encoding the potent embryonic and tumour growth factor Igf2. We show that biallelic *Igf2* supply potentiates a previously unreported *Pten*$^{+/-}$ placental phenotype and results in strain-dependent cardiac hyperplasia and neonatal lethality. Importantly, we also show that the effects of Pten loss *in vivo* are modified by *Igf2* supply, as lack of *Igf2* results in extended survival and delayed tumour development while biallelic supply is associated with reduced lifespan and accelerated neoplasia in females. Furthermore, we demonstrate that reduction of PTEN protein to heterozygote levels in human MCF7 cells is associated with increased proliferation in response to IGF2, and does not result in desensitisation to IGF2 signalling. These data indicate that the effects of Pten loss at heterozygote levels commonly observed in human tumours are modified by Igf2 ligand, and emphasise the importance of the evaluation of upstream pathways in tumours with *Pten* loss.
Oncogene (2012) **31,** 3635–3646; doi:10.1038/onc.2011.526; published online 28 November 2011

Keywords: PTEN; IGF2; Cowden syndrome; imprinting; placenta; mammary gland

Introduction

PTEN is a dual specificity phosphatase that acts as a key negative regulator of the ligand-activated PI3K-Akt pathway (Carracedo and Pandolfi, 2008). PTEN acts to dephosphorylate phosphatidyl inositol (3,4,5) triphosphate to the diphosphate (4,5), thus reducing activation of Akt. Germline mutations in *PTEN* cause Cowden syndrome (OMIM 158350), characterised by hamartomas and increased risk of cancer of the breast, thyroid and endometrium, and somatic mutation and epigenetic silencing of *PTEN* occur at high frequency in sporadic tumours (for example, COSMIC database http://www.sanger.ac.uk/genetics/CGP/cosmic/). *Pten*$^{+/-}$ mice develop hyperplastic and neoplastic change in multiple organs from 3 months of age and typically die at <15 months from tumours or autoimmune disease (Di Cristofano *et al*., 1998; Podsypanina *et al*., 1999; Wang *et al*., 2010). These phenotypes are potentiated by reduced Pml, Cdkn2a or Tsc2 dosage (Di Cristofano *et al*., 2001; Ma *et al*., 2005; Manning, 2005; Trotman *et al*., 2006) and partially ameliorated by a decrease in downstream components of the PI3K-Akt pathway such as Akt1, Pdk1 and Rictor (Bayascas *et al*., 2005; Chen *et al*., 2006; Guertin *et al*., 2009). In contrast, upstream Grb2 heterozygosity does not modify *Pten*$^{+/-}$ tumour development (Cully *et al*., 2004), indicating selective requirement of additional signalling components in *Pten*$^{+/-}$-associated tumourigenesis.

Insulin-like growth factor 2 (IGF2) is a potent embryonic growth factor with homology to IGF1 that signals through IGF1R and insulin receptor isoform A to activate the PI3K-Akt and mitogen-activated protein kinase pathways (Foulstone *et al*., 2005). The supply of IGF2 ligand is tightly regulated, with one mechanism being genomic imprinting of *Igf2* both in human and

Correspondence: Professor AB Hassan, Sir William Dunn School of Pathology, University of Oxford, South Parks Road Oxford, Oxford OX1 3RE, UK.
E-mail: bass.hassan@path.ox.ac.uk
[5]Current address: National Heart and Lung Institute, University College London, Imperial College Hammersmith Hospital, Du Cane Road, London W12 0NN, UK
Received 16 March 2011; revised 28 August 2011; accepted 9 October 2011; published online 28 November 2011

mouse. Imprinting restricts *Igf2* expression to the paternal allele with reciprocal maternal expression of a non-coding RNA (ncRNA) *H19* (Bartolomei *et al*., 1991; DeChiara *et al*., 1991). Coordinate expression of *Igf2* and *H19* on each allele is regulated by a differentially methylated intergenic imprinting control region (ICR) and competition for shared downstream enhancers between the two loci (Bell and Felsenfeld, 2000). Loss and gain of function of *IGF2* contribute to the human growth disorders Silver-Russell (OMIM #180860) and Beckwith-Wiedemann (OMIM #130650) syndromes, respectively. In the mouse, paternal inheritance of an *Igf2* null allele (*Igf2*$^{-p}$) is associated with approximately 1% wild-type (wt) levels of *Igf2* expression and results in foetoplacental growth restriction (60% wt) (DeChiara *et al*., 1991). In contrast, maternal inheritance of a 13 kb *H19*/ICR deletion (*H19*$^{-m}$) results in both loss of ncRNA and biallelic *Igf2* expression, *Igf2* mRNA levels of 127–219% wt and foetal (127%) and placental (140%) overgrowth (Leighton *et al*., 1995). Loss of imprinting of *IGF2* is common in human cancers (van Roozendaal *et al*., 1998; Cui *et al*., 2002) and murine studies have confirmed that *Igf2* is required for tumour progression in the RIP-TAg pancreatic (Christofori *et al*., 1994), *Apc*^{Min} intestinal (Hassan and Howell, 2000) and the *Ptch*$^{+/-}$ medulloblastoma models (Corcoran *et al*., 2008), whereas biallelic *Igf2* supply in combination with *Apc*^{Min} promotes adenoma progression (Sakatani *et al*., 2005; Harper *et al*., 2006). Recently, growth regulatory and tumour suppressive roles for *H19* have been established (Yoshimizu *et al*., 2008; Gabory *et al*., 2009), and tumour-promoting miRNA (micro RNA) within the *Igf2* (miR-483*) and *H19* (miR-675-3p) loci reported (Tsang *et al*., 2010; Veronese *et al*., 2010).

As a negative regulator of the PI3K-Akt pathway, PTEN performs a pivotal role in the regulation of IGF2 signalling, and several lines of evidence indicate a complex interplay between IGF2 and PTEN in normal tissues and tumours. *Pten* expression is induced in response to IGF2 ligand supply, generating negative feedback loops dependent on Egr1 and IGFBP2 (Moorehead *et al*., 2003; Perks *et al*., 2007). Moreover, evidence in human glioblastomas with PTEN loss indicates that *IGF2* overexpression promotes tumour growth, suggesting that the two may cooperate in tumour development (Soroceanu *et al*., 2007). However, desensitisation of IGF signalling can occur following either PI3 K activation or PTEN loss through feedback mechanisms that include regulation of IGF1R levels, insulin receptor substrate (IRS)-1 stability, regulation of IRS2 and inhibition of IRS-1 by protein kinase C (PKC)ζ (Liu *et al*., 2001; Ravichandran *et al*., 2001; Lackey *et al*., 2007). Collectively, these data suggest that although subtle changes in *Igf2* and *Pten* expression may autoregulate through feedback mechanisms, such compensation is inadequate to prevent the effects of allelic dosage variation of either gene in the mouse (DeChiara *et al*., 1991; Leighton *et al*., 1995; Di Cristofano *et al*., 1998; Podsypanina *et al*., 1999) and raise the possibility that combined dysregulation may cooperate in tumour promotion. However, at present the *in vivo* dependency of *Pten*$^{+/-}$-associated tumourigenesis on *Igf2* supply remains unclear. Here, we sought to address this question by the generation of *Pten*$^{+/-}$ mice with differing *Igf2* allelic dosage, resulting in compound mutants with either normal, substantially decreased or approximately doubled *Igf2* expression.

Results

Igf2 *and* Pten *regulate placental growth and organisation*

We first evaluated the interactions of *Igf2* and *Pten* by mating mutant mice on a C57BL/6 background to generate wt, *Pten*$^{+/-}$, *H19*$^{-m}$, and *H19*$^{-m}$, *Pten*$^{+/-}$ compound mutant progeny. The expected foetoplacental overgrowth of *H19*$^{-m}$ mutants was evident by E12.5 and persisted throughout gestation (Figures 1a and b). Unexpectedly, we also detected an increase in *Pten*$^{+/-}$ foetal and placental weights by E15.5 (119% and 123% wt, respectively, $P<0.001$ both comparisons) that subsequently diminished in the foetus by E18.5 (107% wt, $P=$NS) but persisted in the placenta (122% wt, $P<0.001$). *H19*$^{-m}$, *Pten*$^{+/-}$ compound mutants were, in turn, larger than either class of single mutant (Figures 1a and b), though the combination was less than additive in the foetus (131% wt at E15.5 and E18.5) and greater than additive in the placenta (165% and 180% wt, $P<0.001$ vs all groups) (Figures 1a and b).

An approximate doubling of *Igf2* mRNA in *H19*$^{-m}$ and *H19*$^{-m}$, *Pten*$^{+/-}$ mutant placentas was associated with a relatively smaller increase in protein (Figure 1c, Supplementary Figures S1a and b), whereas *Pten* expression and protein in *Pten* heterozygotes were half and two thirds wt level, respectively, and independent of Igf2 (Figure 1d, Supplementary Figures S1c and d). As expected, the decrease in Pten protein was accompanied by an increase in Ser473-phosphorylated Akt (p-Akt^{S473}) in both *Pten*$^{+/-}$ and *H19*$^{-m}$, *Pten*$^{+/-}$ mutants (Figure 1d), though importantly, no additional effect of biallelic *Igf2* expression was detected on Akt and Erk 1/2 activation. We next evaluated localisation of the placental growth effects. The murine placenta can be divided into three zones; the part-maternally derived decidua; the junctional zone, comprising spongiotrophoblast (Sp) and glycogen cells (Gly); and the labyrinth (Lab), which contains foetal and maternal vessels and is the site of nutrient exchange. Overgrowth of *H19*$^{-m}$ placentas was largely associated with preservation of placental architecture, whereas *Pten*$^{+/-}$ mutants displayed tortuosity of the Sp/Lab interface by E15.5 with expansion of the junctional zone (31.48 ± 1.7 vs 25.7 ± 1.68% in wt) (Figures 1e and f).

Biallelic *Igf2* supply potentiated both *Pten*$^{+/-}$ placental phenotypes, with marked abnormality of the Sp/Lab border and greater increase in the size of the junctional zone (34.8 ± 3.49%, $P<0.05$ vs wt) in *H19*$^{-m}$, *Pten*$^{+/-}$ placentas (Figures 1e and f). Gly cells are known to be Igf2 dependent (Lopez *et al*., 1996; Carter *et al*., 2006; Esquiliano *et al*., 2009) and, as anticipated, were present in increased numbers at E18.5 in *H19*$^{-m}$ placentas,

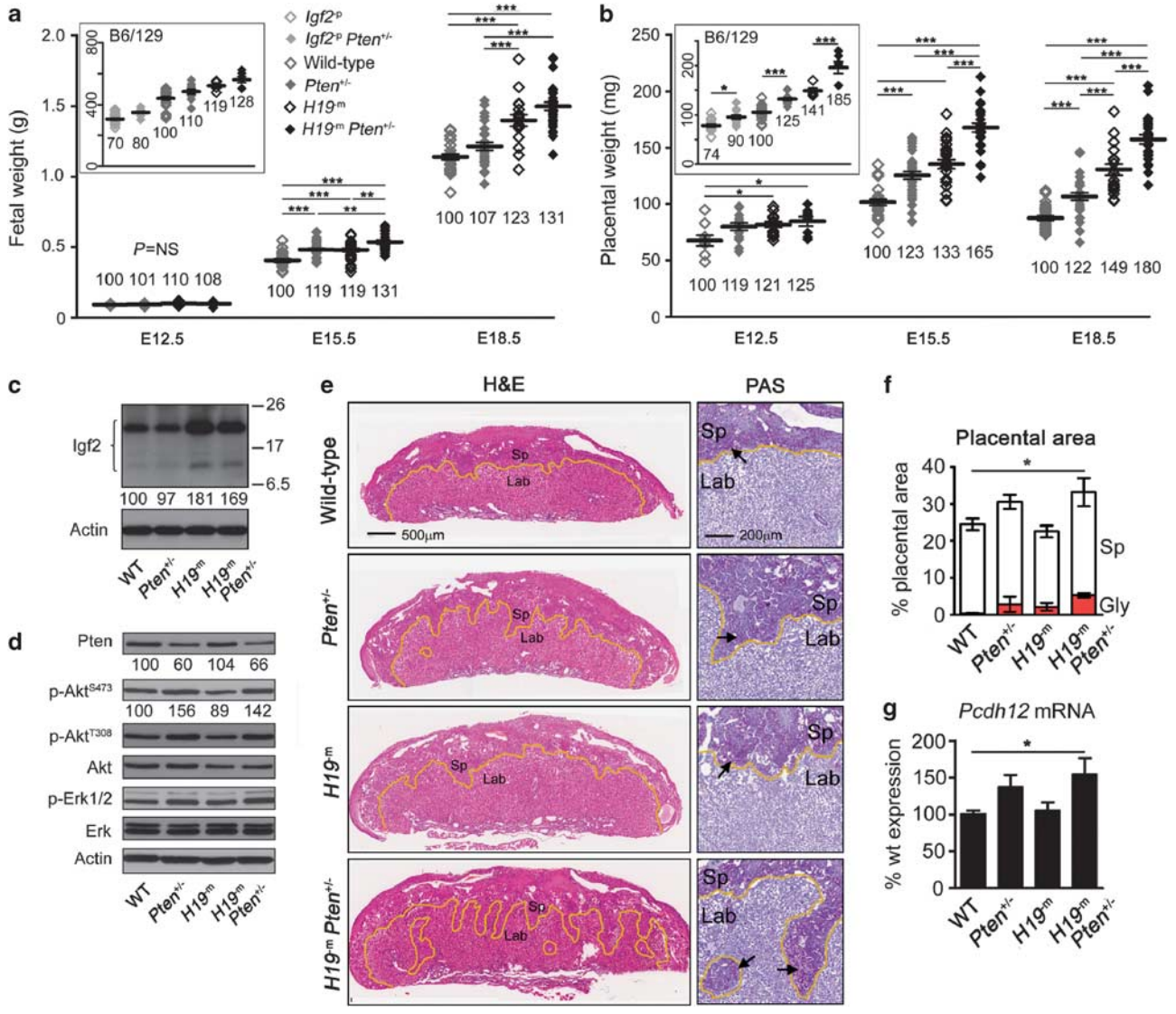

Figure 1 *Igf2* and *Pten* regulate foetoplacental growth, Sp and Gly cells. (**a**, **b**) Fetal (**a**) and placental (**b**) weights by embryonic stage on a C57BL/6 background (main panel) and on an F1 hybrid C57BL/6/129S2 background at E15.5 (insets). Numbers below columns indicate weights as % of wt, numbers on *y* axis in insets indicate weights in mg. (**c**) Igf2 immunoblot of littermate E15.5 placental lysates. Multiple bands correspond to the 22 kDa, 156 residue pro-peptide and the 11–17 kDa, 87 and 104 residue 'big' forms described in human, which undergo variable glycosylation. The mature 7.5 kDa 67-residue peptide was not detected in placental tissue. Numbers below bands indicate % of wt level (quantified by densitometry in Supplementary figure S1b), to the right represent molecular weights in kDa. (**d**) Immunoblot of littermate E15.5 placental lysates for indicated proteins. Numbers below bands indicate levels as % of wt (quantified by densitometry in Supplementary figure S1d). (**e**) Littermate placental sections at E18.5. To the left are low magnification haematoxylin and eosin-stained sections, higher magnification panels to the right show staining with periodic acid Schiff. Sp and Lab are indicated, and the Sp/Lab interface highlighted (yellow line). Note disorganisation of Sp/Lab interface in *Pten*$^{+/-}$ and *H19*$^{-m}$*Pten*$^{+/-}$ mutants. periodic acid Schiff staining demonstrates persistent Gly cells in all mutant classes most prominent and abnormally localised in *H19*$^{-m}$*Pten*$^{+/-}$ placenta (pink cells indicated by arrows, right panels). Images are representative of $\geqslant 5$ placentas examined in each class. (**f**) Quantification of proportion of Sp and Gly as percentage of placenta determined by point counting. (**g**) Expression of Gly cell marker *Pcdh12* in E15.5 placenta assayed by RT–qPCR. Error bars in (a, b, f, g) indicate ± s.e.m. from $\geqslant 5$ biological replicates. *, ** and *** indicate $P<0.05$, <0.01 and <0.001, respectively.

though interestingly at lower levels than in *Pten*$^{+/-}$ mutants (Figure 1f). This indication of Gly cell regulation by Pten was supported by an increased expression of the Gly cell marker *Pcdh12* (Coan *et al*., 2006) in *Pten*$^{+/-}$ placentas (137% wt, $P=$NS) (Figure 1g). Combined dysregulation in *H19*$^{-m}$, *Pten*$^{+/-}$ placentas was accompanied by further increase in Gly cell number and *Pcdh12* expression (154% wt, $P<0.05$) (Figures 1f and g), and markedly abnormal distribution of Gly cells throughout the Lab and Sp was confirmed with staining by Periodic acid-Schiff (Figure 1e). Immunohistochemistry demonstrated an apparent reciprocal distribution for Pten and Igf2 in subcellular regions of the placenta with increased labelling for

activated Akt in the Sp (Supplementary Figures S1e and f) Examination of proliferation in the Lab using ki67 was increased by E18.5 in placentas with biallelic *Igf2* supply, consistent with their increased relative overgrowth in late gestation (Supplementary Figure S1g).

We next generated mice with varying allelic dosage of *Igf2*: null (*Igf2*$^{-p}$), monoallelic or biallelic expression and either wt or heterozygous *Pten* supply on a uniform F1 hybrid C57BL/6/129S2 background. This both reproduced the growth effects and confirmed that the *Pten*$^{+/-}$ foetoplacental phenotype persisted despite near complete absence of Igf2 (Supplementary Figures S2a–c).

Biallelic Igf2 *supply combined with* Pten$^{+/-}$ *results in cardiac hyperplasia and neonatal lethality*

By postnatal day 10 on a C57BL/6 background, a deficit of *H19*$^{-m}$,*Pten*$^{+/-}$ compound mutants was evident (49% of expected, $P<0.0001$). This was greater in females than males (29% of expected, $P<0.001$ vs 64%, $P=$NS) (Supplementary Figure S3a). A significant and disproportionate increase in heart weights in *H19*$^{-m}$,*Pten*$^{+/-}$ female neonates (Supplementary Figure S3b) was absent at postnatal day 5, by which time the deficit was evident. Magnetic resonance imaging at E15.5 (Supplementary Figure S3c) demonstrated that the increased weight of *H19*$^{-m}$,*Pten*$^{+/-}$ hearts was mirrored by changes in biventricular volume and interventricular septal thickness (Supplementary Figures S3d and e). Additionally, two *H19*$^{-m}$,*Pten*$^{+/-}$ foetuses demonstrated a marked dilatation and thinning of the ventricular myocardium (Supplementary Figure S3c). Collectively, these data suggested an association between the cardiac abnormalities and lethality. Quantification of cardiomyocyte density demonstrated growth because of hyperplasia (Supplementary Figure S3f), and analysis confirmed expected *Igf2* and *Pten* mRNA and protein levels in mutant hearts (not shown). As cardiac abnormalities may result from placental defects, we re-examined *H19*$^{-m}$,*Pten*$^{+/-}$ placentas by sex, but found no differences between males and females (not shown). Surviving *H19*$^{-m}$,*Pten*$^{+/-}$ mutants did not display any signs of cardiac failure, and *in vivo* assay of heart function by dynamic magnetic resonance imaging at postnatal day 30 demonstrated no obvious left ventricular impairment (not shown). However, necropsy of adults (>3 months) revealed cardiomegaly in both *Pten*$^{+/-}$ and *H19*$^{-m}$,*Pten*$^{+/-}$ animals, though in contrast to neonates this was more marked in compound mutant males (Supplementary Figures S3g–i).

Igf2 *modifies* Pten$^{+/-}$ *survival*

We next examined the effects of *Igf2* supply on the survival of adult *Pten*$^{+/-}$ mice by generation of F1 hybrid C57BL/6/129S2 compound mutants with null, monoallelic or biallelic *Igf2* expression. Animals were sacrificed on development of either external tumours of >10 mm diameter, signs of illness or at the study endpoint of 450 days. Lack of *Igf2* in *Pten*$^{+/-}$ mice was associated with significantly extended lifespan (*Igf2*$^{-p}$, *Pten*$^{+/-}$ median 426 days) compared with *Pten*$^{+/-}$ (359 days) and *H19*$^{-m}$,*Pten*$^{+/-}$ (322 days) animals (Figures 2a–c). This was largely because of effects in females where these differences were greater (373 days, 305.5 days and 274.5 days, respectively, $P=0.0008$ and $P<0.0001$), and a significant decrease in survival with biallelic vs monoallelic *Igf2* expression was also observed (Figure 2c). Lifespan of males was longer as anticipated (Manning, 2005), and did not vary significantly between groups (Figure 2b). No deaths occurred in any *Pten* wt animal ($n=73$) irrespective of *Igf2* dose.

Igf2 *modifies* Pten$^{+/-}$ *epithelial tumourigenesis in multiple organs*

We analysed the effects of *Igf2* on *Pten*$^{+/-}$ tumourigenesis. Large (>10 mm) external tumours developed significantly earlier in *H19*$^{-m}$,*Pten*$^{+/-}$ (median 323 days) than *Pten*$^{+/-}$, or *Igf2*$^{-p}$,*Pten*$^{+/-}$ mice (median not reached, Figures 2d–f). The difference in tumour onset by *Igf2* in *Pten*$^{+/-}$ males (Figure 2e) was significant only for comparison of *Igf2* null with biallelic mutants. However, variation in females was larger and highly significant for all comparisons (Figure 2f). External tumours were predominantly hyperplastic lymph nodes, mammary carcinomas and, less frequently, lymphomas. Clinically detectable (>5 mm) *Pten*$^{+/-}$ lymphadenopathy was accelerated with biallelic *Igf2* expression and delayed in the *Igf2*$^{-p}$,*Pten*$^{+/-}$ cohorts (Supplementary Figures S4a–c). Furthermore, histopathological analysis demonstrated a tendency to higher-grade lymphoid lesions with *Igf2* gain of function (Supplementary figures S4d–g).

We next focused on the effects of variation of *Igf2* allelic supply on epithelial gene expression and tumourigenesis. RT–qPCR (reverse transcriptase-quantitative PCR) on mammary glands, endometria and prostates of virgin animals of 6–8-weeks age confirmed that although *Igf2* expression was reduced to approximately 1% of the levels of E9.5 embryos, it remained detectable and was substantially reduced in *Igf2*$^{-p}$ mutants (1–8% wt), and doubled in *H19*$^{-m}$ mutants (178.9–200% wt) (Supplementary Figures S5a–c). *H19* expression was greatly reduced in *H19*$^{-m}$ mutants, though no significant change was found in tissues from *Igf2*$^{-p}$ animals and no alteration in *Pten* expression with change in *Igf2* supply was detected (Supplementary Figures S5d–f).

Clinically detectable mammary carcinomas in females occurred significantly later in *Igf2*$^{-p}$,*Pten*$^{+/-}$ mutants than both *Pten*$^{+/-}$ and *H19*$^{-m}$,*Pten*$^{+/-}$ groups. These data were combined with systematic analysis of macroscopically normal female mammary glands (see Supplementary methods) to determine the true incidence and timing of mammary neoplasia. A trend towards fewer carcinomas in *Igf2*$^{-p}$,*Pten*$^{+/-}$ mutants (Figure 3a) was accompanied by a significant delay in tumour onset (Figure 3b). Carcinomas were histologically similar in all cohorts with prominent stromal component (Figure 3c), with no differences in proliferation by ki67 labelling (not shown). No metastases were detected in any group. No pathological changes were observed in *Pten* wt female ($n=6$) or *Pten*$^{+/-}$ male ($n=30$)

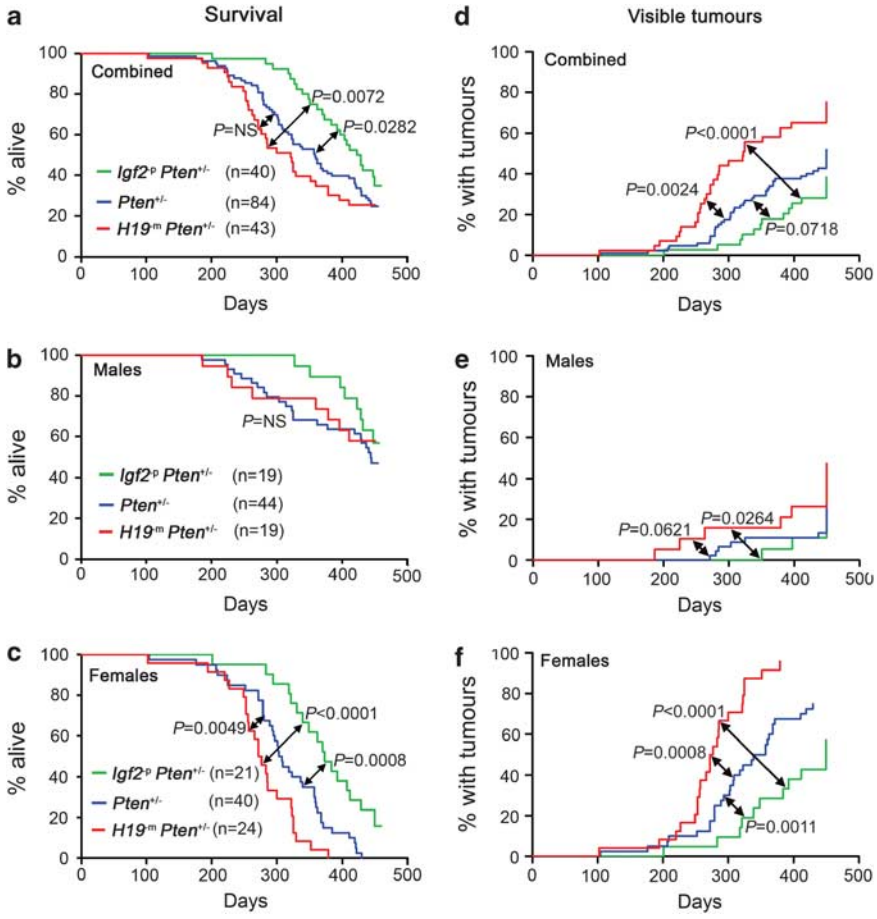

Figure 2 *Igf2* allelic dose modifies survival and tumour development in *Pten*$^{+/-}$ mice. (**a–c**) Survival of *Pten*$^{+/-}$ mice by *Igf2* allelic dosage. Percentage of total (**a**), male (**b**) and female (**c**) populations alive by time. No deaths occurred in *Pten* wt controls ($n=73$). Note the female-predominant effect (**c**). (**d–f**) Incidence of large (>10 mm) external tumours. Percentage of total (**a**), male (**b**) and female (**c**) populations with tumours by time. The total includes only external tumours during the study period of 450 days and visceral tumours detected at necropsy at study endpoint. Tumours were predominantly hyperplastic lymph nodes, lymphomas and mammary carcinomas.

mammary glands, irrespective of *Igf2* dose. Endometrial hyperplasia was common in all in *Pten*$^{+/-}$ groups, though strikingly no case of progression to carcinoma was detected in *Igf2*$^{-p}$,*Pten*$^{+/-}$ females, in contrast to 5/24 (21%) *Pten*$^{+/-}$ and 4/23 (17%) *H19*$^{-m}$,*Pten*$^{+/-}$ animals (Figure 3d). Thus, lack of *Igf2* was associated with a significant delay in carcinoma onset (Figures 3e,f), although these animals were killed for other indications. Although murine prostatic intraepithelial neoplasia (mPIN) was near-universal in all *Pten*$^{+/-}$ classes, mPIN was detected significantly earlier in *H19*$^{-m}$,*Pten*$^{+/-}$ males and there was a trend towards fewer Grade 4 lesions in the *Igf2*$^{-p}$,*Pten*$^{+/-}$ cohort (Figures 3g–i). Ki67 index in neoplastic endometrial and prostatic lesions did not vary between groups, and patterns of Pten loss and Akt activation were similar (not shown). Though common in all *Pten*$^{+/-}$ mutants, intestinal polyps were significantly smaller in animals lacking *Igf2* (*Igf2*$^{-p}$,*Pten*$^{+/-}$ 3.1 ± 0.3 mm; *Pten*$^{+/-}$ 4.0 ± 0.2 mm; *H19*$^{-m}$,*Pten*$^{+/-}$ 3.9 ± 0.2 mm, $P<0.05$ vs *Pten*$^{+/-}$). Phaeochromocytoma was fully penetrant in all *Pten*$^{+/-}$ groups.

Promotion of mammary tumourigenesis by Igf2 *combined with decreased Pten protein*

We next sought to examine the effect of *Igf2* effect on mammary tumourigenesis. Despite the extended life span of *Pten*$^{+/-}$ females lacking *Igf2*, mammary tumours in this group remained smaller than other mutants (Figure 4a). Conversely, tumour multiplicity tended to increase with gain of *Igf2* alleles (Figure 4b). Mammary hyperplasia, a preneoplastic lesion (Supplementary Figure S6a), was detected at similar frequency in females of all genotypes (Figure 3a), suggesting that *Igf2* may promote the transition to carcinoma in *Pten*$^{+/-}$ females. RT–qPCR confirmed that *Igf2* expression in mammary carcinomas corresponded with *Igf2* allelic dose (Figure 4c). As in the normal mammary gland, *H19* expression was substantially decreased in *H19*$^{-m}$,*Pten*$^{+/-}$ mutant carcinomas (Supplementary Figure S6b). Levels of *Pten* mRNA in tumours relative to wt mammary gland were reduced by a similar degree in all genotypes ($P=$NS) (Figure 4d). There was no evidence of feedback downregulation of *Igf1r* secondary to this (Supplementary Figure S6c), though interestingly *Igf1*

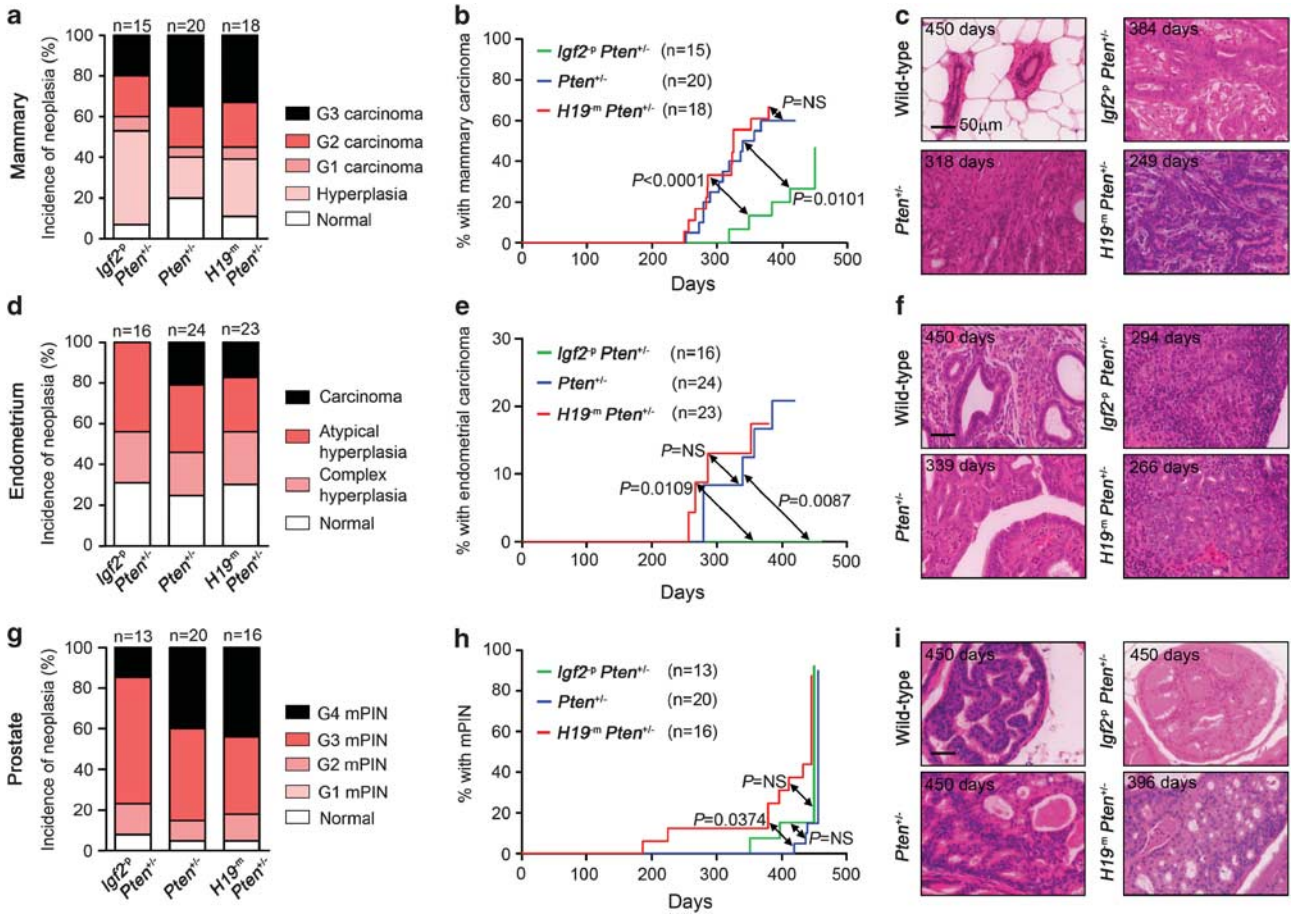

Figure 3 *Igf2* allelic dose modifies *Pten*$^{+/-}$ epithelial neoplasia. (**a–c**) Mammary pathology in *Pten*$^{+/-}$ mice by *Igf2* supply. Incidence (**a**) and latency (**b**) of mammary carcinoma in virgin females. (**c**) Representative images of normal wt female mammary gland and Grade 3 tumours in each mutant class, illustrating the prominent stromal component of lesions. (**d–f**) Endometrial pathology in *Pten*$^{+/-}$ mice by *Igf2* supply. Frequency (**d**) and latency (**e**) of endometrial hyperplasia/carcinoma with representative images (**f**) of normal wt endometrium and the highest grade lesions detected in each mutant genotype (*Igf2*$^{-p}$*Pten*$^{+/-}$ atypical hyperplasia; *Pten*$^{+/-}$ G3 serous adenocarcinoma; *H19*$^{-m}$*Pten*$^{+/-}$ G2 endometrioid adenocarcinoma). (**g–i**) mPIN in *Pten*$^{+/-}$ mice by *Igf2* supply. Incidence (**g**), latency (**h**) and representative images (**i**) of normal wt prostate and Grade 4 mPIN in *Pten*$^{+/-}$ mutants. Numbers in each panel in (**c**, **f** and **i**) indicate the age of animal at the time of killing.

expression was low in *Pten*$^{+/-}$ and *H19*$^{-m}$,*Pten*$^{+/-}$ mammary carcinomas (Supplementary Figure S6d). Notably, despite similar *Pten* expression, immunoblot analysis demonstrated a significant progressive decrease in tumour Pten protein with increasing *Igf2* allelic dose (Figures 4e and f). Associated Akt phosphorylation was universal (Figure 4e, Supplementary Figures S6e and f), and a trend to greater Akt activation with *Igf2* gain of function was mirrored by a greater nuclear exclusion of FoxO1, a readout of PI3K-Akt pathway activity (Supplementary Figure 6g). Immunohistochemistry demonstrated foci of epithelial Pten loss in a minority of advanced lesions only (Figure 4g), insufficient in extent to fully explain the relative reduction in total protein.

Perturbation of miR-483 and miR-675-3p in* Igf2^{-p} *and* H19^{-m} *mutants*

Given the recent demonstration of tumour-promoting functions for miR-483 and miR-675, we next assessed whether their perturbation in *Igf2*$^{-p}$ and *H19*$^{-m}$ mutants was likely to have contributed to the modification of phenotype. Using E9.5 embryos, selected for their high expression of *Igf2* and *H19* (Burns and Hassan, 2001), we confirmed the expected changes in *Igf2* expression in *Igf2*$^{-p}$ and *H19*$^{-m}$ embryos (0.8%, and 246.6% wt, respectively) (Figures 5a and b). We next examined changes in miRNA expression in both classes of mutant using Ilumina 96-assay universal array matrix miRNA arrays.

miR-483* is located within the second intron of *Igf2* in a region of the gene spared by the targeting construct used in this study (DeChiara *et al*., 1990). We anticipated an increase in miR-483* levels in *H19*$^{-m}$ mutants of similar magnitude to that of *Igf2*, but surprisingly this was not the case (105.1% wt, $P = \text{NS}$). Also unexpected was an upregulation of miR-483* in *Igf2*$^{-p}$ mutants (107.3% wt) (Figure 5c). Importantly, no correlation between *Igf2* and miR-483* expression was detected ($R^2 = 0.365$, $P = \text{NS}$). miR-675-3p is located within the first exon of *H19*, which is deleted along with

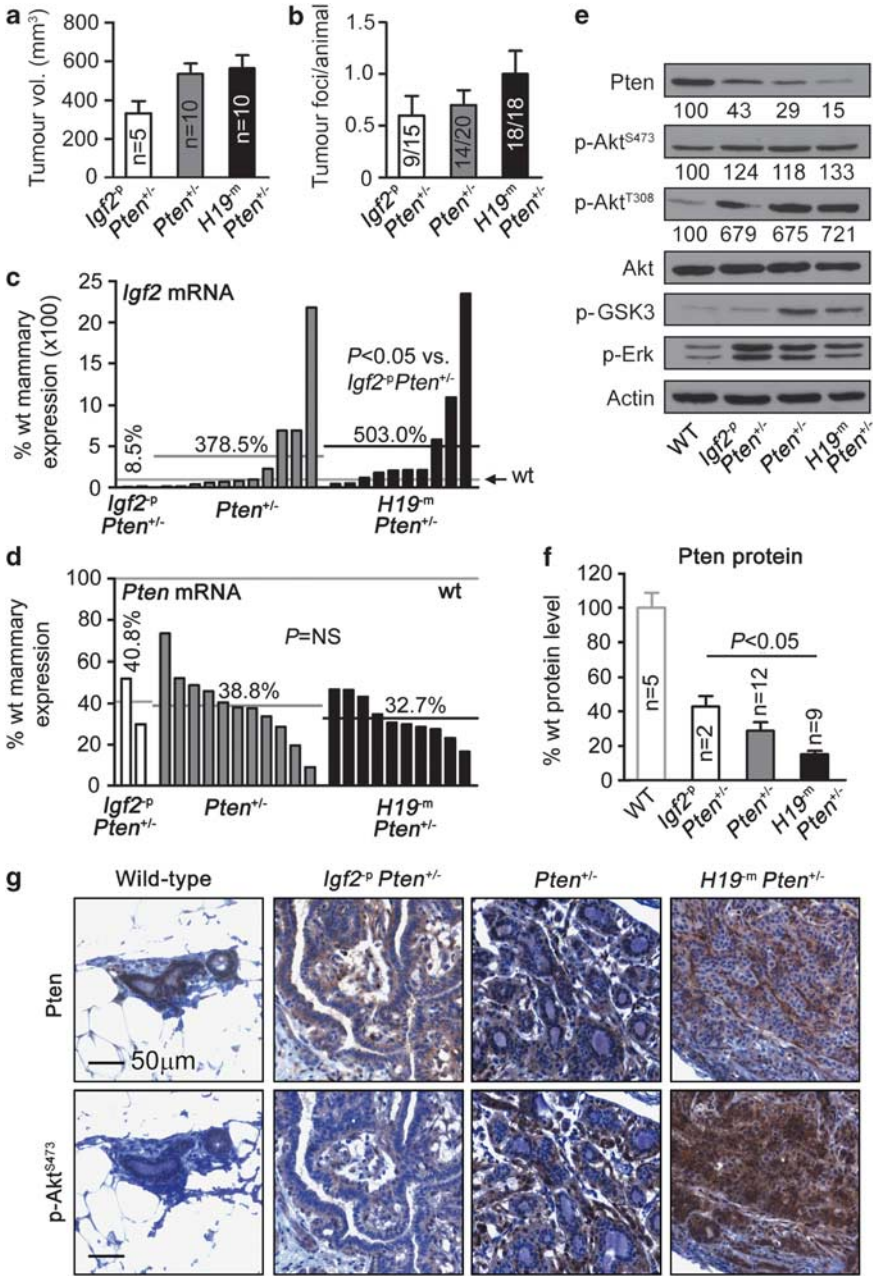

Figure 4 *Igf2* promotes *Pten*$^{+/-}$ mammary tumourigenesis. (**a**, **b**) Mean mammary tumour volume (**a**) and mean number of tumour foci per animal (**b**) by *Igf2* allelic dose. (**c**, **d**) Waterfall plots showing expression of *Igf2* (**c**) and *Pten* (**d**) in mammary carcinomas (only two tumours in *Igf2*$^{-p}$*Pten*$^{+/-}$ mutants were of sufficient size to obtain tissue for RNA and protein analysis in addition to fixation). Horizontal lines indicate wt level (light grey) and mean expression of each mutant class (black), with percentage values relative to wt mammary gland. Expression was elevated >2-fold in 4/11 *Pten*$^{+/-}$ and 6/10 *H19*$^{-m}$*Pten*$^{+/-}$ mutants. (**e**, **f**) Immunoblot of mammary tumor lysates (**e**) showing progressive decrease in Pten protein with increasing *Igf2* allelic dose, quantified by densitometry in (**f**). Numbers below bands in (**e**) indicate protein level as % of wt mammary gland from densitometry in (**f**) and Supplementary Figures S6e and f. Note the increase in p-Akt^{T308} relative to p-Akt^{S473}. (**g**) Immunohistochemistry demonstrated infrequent foci of complete epithelial Pten loss in advanced lesions only. Error bars in (**a**,**b** and **f**) represent ± s.e.m. Statistical comparisons in (**c**, **d** and **f**) are between *Pten*$^{+/-}$ mutant classes.

10 kb of 5′ flanking sequence containing the DMR in the Δ*H19*/DMR mutant allele (Leighton *et al*., 1995). As expected, *H19*$^{-m}$ mutants showed a significant decrease in miR-675-3p expression (78.1% wt, $P<0.001$), though this was smaller than the reduction in *H19* ncRNA (Figure 5d). Notably, miR-675-3p expression was unchanged in *Igf2*$^{-p}$ mutants (99.6% wt, $P=$NS) (Figure 5d). Changes in the expression of 377 additional miRNAs analysed were modest and are listed in Supplementary Table S1. Aside from miRNA perturbations that we could attribute to expression of the neomycin resistance gene, we observed a number of

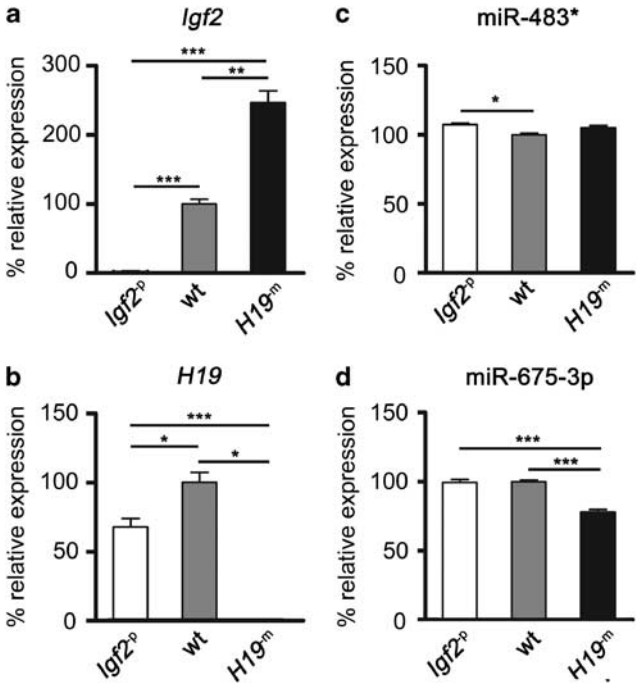

Figure 5 Perturbation of miR-483* and miR-675-3p associate with *Igf2* and *H19*/DMR deletions. Quantification of (**a**) *Igf2*, (**b**) *H19*, (**c**) miR-483* and (**d**) miR-675-3p expression in E9.5 embryos by RT–qPCR (**a**, **b**) and Illumina array (**c**, **d**). Results are shown as percentage of wt levels. Error bars represent ± s.e.m. of 14–28 biological replicates per group. *, ** and *** indicate $P<0.05$, <0.01 and <0.001, respectively.

miRNAs deregulated to similar extents in mutants as miR-483* and miR-675-3p. Importantly, no miRNA significantly downregulated in *Igf2*$^{-p}$ embryos demonstrated significant upregulation in *H19*$^{-m}$ embryos, or vice versa.

Reduction of PTEN protein to heterozygote levels in human breast cancer cells associated with increased IGF2-mediated proliferation

PTEN loss has previously been shown to cause desensitisation to IGF1 and insulin signalling (Lackey *et al*., 2007). To reconcile these results with our data, and to examine the interaction between IGF2 and PTEN loss in a system free from *H19* ncRNA, miR-483* and miR-675-3p perturbation, we used shRNA (small hairpin RNA) to reduce *PTEN* expression to heterozygote levels in MCF7 human breast cancer cells. PTEN protein in MCF7 cells with partial PTEN knockdown (MCF7$^{PTEN\ KD}$) was 61% that of MCF7 cells expressing control shRNA (MCF7^{CTRL}) (Figures 6a and b). As anticipated, reduced PTEN in MCF7$^{PTEN\ KD}$ cells was accompanied by increased Akt activation (Figure 6a). Importantly, no changes in levels of total IGF1R, total IRS1 (Figure 6a) or inhibitory Ser-612 phosphorylated IRS1 (not shown) were detected. Following IGF2 stimulation, both MCF7^{CTRL} and MCF7$^{PTEN\ KD}$ cells demonstrated similar IGF1R-PI3K-Akt and mitogen-activated protein kinase pathway activation as demonstrated by comparable levels of

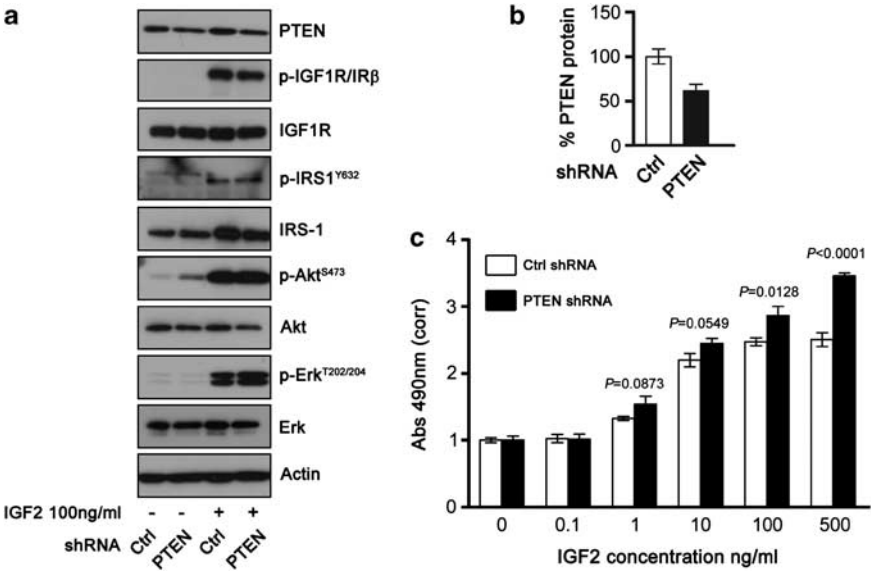

Figure 6 Reduction of PTEN protein to heterozygote levels sensitises MCF7 cells to mitogenic effect of IGF2. (**a**) MCF7 human breast cancer cells with stable expression of either scrambled control (Ctrl) or anti-PTEN shRNAs were serum starved overnight and then stimulated with recombinant human IGF2 at 100 ng/ml. Lysates were prepared at baseline and after 2 hours following treatment, and immunoblotting for the proteins indicated performed. (**b**) Densitometry quantification of the reduction in PTEN protein (without IGF2 stimulation) from (**a**). (**c**) Proliferation of MCF7 cells expressing either control or anti-PTEN shRNA in serum-free medium following stimulation by IGF2. Exogenous ligand was indicated at the concentrations indicated, and absorbance measured after 48 h by MTS assay. Results are normalised to the values in controls treated with vehicle alone. Error bars indicate ± s.e.m. of at minimum six replicates per dose. Data in (**a**) and (**b**) are representative of experiments performed in duplicate and triplicate, respectively.

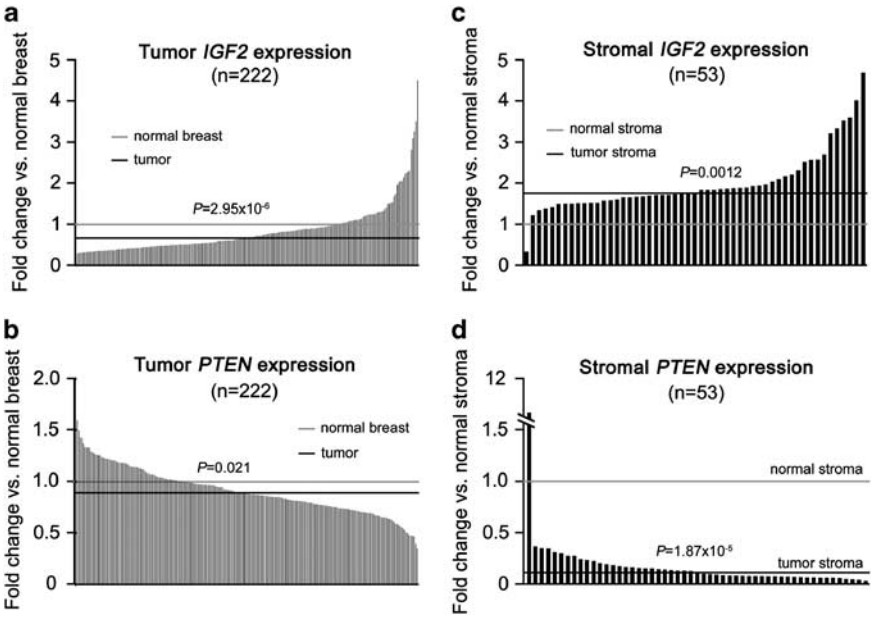

Figure 7 *IGF2* and *PTEN* microarray expression in human breast carcinoma. Human breast cancer data sets suggest stromal role of *IGF2* and *PTEN* dysregulation. *IGF2* (**a**, **c**) and *PTEN* (**b**, **d**) expression in whole breast carcinomas compared with normal breast tissue (222 tumours and 10 normal breast pools) (**a**, **b**), and tumour stroma compared with normal stroma (53 tumour and 12 normal samples) (**c**, **d**). Grey lines show median expression in normal breast/breast stromal samples and black lines median expression in breast tumour/breast tumour stroma.

activated IGF1R (p-IGF1R^{Y1131}), IRS1 (p-IRS-1^{Y632}), Akt (p-Akt^{S473}) and Erk1/2 (p-Erk$^{T202/204}$) (Figure 6a).

It has also been shown in MCF7 cells that high concentrations of IGF2 result in relative inhibition of cellular proliferation through feedback induction of PTEN (Perks *et al*., 2007). We next assessed whether partial PTEN knockdown abrogated this autoregulation. Stimulation of MCF7^{CTRL} and MCF7$^{PTEN\ KD}$ cells with increasing concentrations of IGF2 confirmed the mitogenic effect of recombinant ligand at concentrations of >1 ng/ml, and as anticipated in MCF7^{CTRL} cells this plateaued at 100 ng/ml (Figure 6c). Notably, MCF7$^{PTEN\ KD}$ cells demonstrated increased proliferation in response to IGF2, most strikingly at high ligand concentrations, with no evidence of a plateau in proliferation (Figure 6c).

Human stromal interaction of IGF2 *and* PTEN

Finally, in light of the apparent promotion of stroma-predominant *Pten*$^{+/-}$ mammary tumours by *Igf2* in the mouse, we evaluated the expression of *IGF2* and *PTEN* in human breast carcinomas. We analysed two microarray data sets with normal and tumour samples, the first comprising a cohort of whole breast tumours (Camps *et al*., 2008) and the second a published breast cancer micro-dissected stroma data set (Finak *et al*., 2008). In whole tumours, *IGF2* overexpression was relatively infrequent with a >2-fold increase in mRNA detected in 5.6% of tumours (Figure 7a). Unlike the mouse mutants, miR-483 expression closely correlated with that of *IGF2* ($R^2=0.6$, $P<2.2\times10^{-16}$) and was in fact reduced in tumours compared with normal breast (88.9%, $P<2.44\times10^{-13}$), whereas miR-675 expression was not significantly altered (98.6%, $P=$NS). Interestingly, the decrease in *PTEN* expression in breast tumours was modest (median 89.1% normal breast), with few tumours showing levels $<50\%$ of normal breast (Figure 7b). In contrast, stromal-specific analysis demonstrated near-universal increase in *IGF2* (median 176%, $P=0.0012$) and decrease in *PTEN* expression (median 11.1%, $P=1.87\times10^{-5}$) in tumour stroma compared with normal stroma (Figures 7c and d).

Discussion

We sought to determine whether variation in Igf2 supply secondary to change in *Igf2* allelic dosage modifies *Pten*$^{+/-}$ tumourigesis in order to evaluate the extent to which the effects of Pten loss *in vivo* are dependent upon upstream signalling. We report several novel findings with respect to development and tumourigenesis.

The *Pten*$^{+/-}$ placental phenotype we describe demonstrates tissue-specific requirements for biallelic *Pten* expression in mammalian development. Although both *Pten*$^{+/-}$ placental overgrowth and Sp disorganisation were increased by biallelic *Igf2* supply, they were not ameliorated in *Igf2* null mutants, and the discrete localisation of Igf2, Pten and p-Akt^{S473} within the placental Lab are consistent with a complex interaction (Coan *et al*., 2006). However, when combined with the *Akt1* null placental phenotype of small size, Sp and Gly cell deficiency (Yang *et al*., 2003), our data indicate that an Igf2-Pten-Akt axis regulates placental development (Lopez *et al*., 1996; Carter *et al*., 2006; Esquiliano *et al*.,

2009). Although placental abnormalities in mouse mutants are frequently more severe on a C57BL/6 background, we confirmed that this is strain independent (Frank *et al*., 2002). We failed to detect quantitative differences in proliferation to explain the placental overgrowth in mid-gestation, and it is plausible that our findings result either from subtle cumulative changes or variation earlier than E12.5 (Burns and Hassan, 2001). The use of conditional *Igf2* and *Pten* alleles may facilitate mechanistic insights into the relationship between upstream *Igf2* expression and localisation and *Pten* loss in the placenta.

It is noteworthy that similar to the placenta, *Igf2* is expressed at high levels in neonatal heart, and recent data suggest an important role for *Igf2* in cardiac development (Li *et al*., 2011). Though conditional deletion of both *Pten* alleles results in cardiac hypertrophy (Crackower, 2002), murine cardiac effects of germline heterozygosity have to the best of our knowledge not previously been described. However, a case of ventricular dilatation has been reported in the human (Reardon *et al*., 2001). The cardiac hyperplasia and neonatal lethality with combined *Igf2* and *Pten* dysregulation we report is consistent with an interaction in heart development, though confirmation of this will require the use of conditional genetics to exclude placental effects.

Igf2 has previously been shown to function as a progression factor or second signal in tumour development (Christofori *et al*., 1994; Hassan and Howell, 2000; Harper *et al*., 2006; Corcoran *et al*., 2008). We demonstrate that the marked reduction of *Igf2* expression (1–8% wt) in *Igf2*$^{-p}$ and more modest increase (179–200% wt) in *H19*$^{-m}$ mutants are associated with respectively a substantial amelioration and lesser potentiation of *Pten*$^{+/-}$ tumourigenesis, consistent with a similar role for *Igf2* in the context of *Pten* haploinsufficiency. It is noteworthy that these changes occurred at relevant levels of *Igf2* expression, in contrast to previous transgenic non-physiological studies (Bates *et al*., 1995). *Pten*$^{+/-}$ mammary tumours typically retain heterozygote levels of Pten protein (Alimonti *et al*., 2010). The progressive decrease in tumour Pten protein with gain of *Igf2* is suggestive of additional post-transcriptional regulatory mechanisms, and contrasts with the previous report of *Pten* upregulation in response to increased Igf2 (Moorehead *et al*., 2003). With respect to other relevant feedback regulation secondary to PTEN loss, such as desensitisation to IGF (Lackey *et al*., 2007), decreased Pten protein in mammary carcinomas was not accompanied by down-regulation of *Igf1r* expression. Moreover, reduction of PTEN to heterozygote levels in MCF7 human breast cancer cells resulted in potentiation of the mitogenic effects of IGF2. These changes were greatest at high doses of ligand, consistent with abrogation of the feedback mechanism of *PTEN* upregulation previously demonstrated (Moorehead *et al*., 2003; Perks *et al*., 2007). Collectively, these data suggest that the effects generated by heterozygote levels of PTEN may still be dependent on upstream ligand.

As noted previously, the *H19* ncRNA has recently been demonstrated to have tumour suppressive activity *in vivo* (Yoshimizu *et al*., 2008), whereas miRNAs in the *IGF2* and *H19* loci; miR-483 and miR-675 respectively, have both been ascribed tumour-promoting effects (Tsang *et al*., 2010; Veronese *et al*., 2010). Although *Igf2* expression across the allelic series increased from 1 to 247%, there was no similar variation of any miRNA. Importantly, loss of *H19* (<1% of wt) was not mirrored by equivalent reduction in miR-675-3p in *H19*$^{-m}$ mutants, and miR-483* expression appeared relatively unchanged. Disruption of miR-483* and miR-675-3p was minimal in *Igf2*$^{-p}$ animals, with no consistent pattern of *H19* dysregulation detected. In addition to these changes, our global analysis shows that many independent miRNA are deregulated in both *Igf2*$^{-p}$ and *H19*$^{-m}$ mutants. Our data cannot exclude selective dysregulation of miR-483* and miR-675-3p in tumours, as the small number of *Igf2*$^{-p}$,*Pten*$^{+/-}$ tumours available precluded meaningful analysis. Definitive *in vivo* assessment of the contribution of the miR-483* and miR-675-3p to phenotype may only be provided by specific conditional deletion of respective loci that modify miRNA expression independent of *Igf2*. However, our *in vitro* data demonstrate the proliferative effects of IGF2 at heterozygote levels of PTEN protein in a system free from *H19*, miR-483* and miR-675-3p perturbation.

IGF2 overexpression by human breast cancer stroma has been postulated to promote neoplastic growth by a paracrine mechanism (Singer *et al*., 1995). We demonstrate that increased *Igf2* mRNA in stroma-prominent *Pten*$^{+/-}$ murine mammary tumours is mirrored by near-universal upregulation of *IGF2* and downregulation of *PTEN* in human breast cancer stroma. The role of stromal Pten in suppression of mammary tumourigenesis has recently been demonstrated (Trimboli *et al*., 2009). Our data suggest that the role of stromal IGF2 in breast cancers merits further examination.

In summary, we show that variation of Igf2 ligand supply is associated with modification of development, survival and tumourigenesis in *Pten*$^{+/-}$ mice, that these changes are unlikely to result from perturbation of the *H19* ncRNA, miR-483* or miR-675-3p, and that IGF2 ligand cooperates with partial PTEN loss to promote breast cancer cell proliferation *in vitro*. Collectively, these data indicate that the effects of Pten loss at heterozygote levels commonly observed in human tumours are modified by Igf2, and emphasise the importance of the evaluation of upstream pathways in tumours with *Pten* loss.

Materials and methods

Mice

Igf2^{tm1Rob} (paternal allele disruption, *Igf2*$^{-p}$) *H19*^{tm1Tilg} (maternal allele disruption *H19*$^{-m}$) and *Pten*^{tm1Rps} (heterozygote *Pten*$^{+/-}$) mice were housed and genotyped by PCR as have been described previously (DeChiara *et al*., 1991; Leighton *et al*., 1995; Podsypanina *et al*., 1999) (see Supplementary Information for details of breeding and primer sequences). All

procedures were approved by the UK Home Office and performed under a Home Office Project license following the University of Oxford ethical committee approval.

Tissue analysis
RT–qPCR, immunoblotting, histology and immunohistochemistry were performed by standard techniques. Full methods are provided in Supplementary Information.

3D Magnetic resonance microscopy
Formalin-fixed foetuses obtained at E15.5 were suspended in phosphate-buffered saline doped with gadolinium diethylenetriaminepentaacetic acid (DTPA) and imaged by high-resolution magnetic resonance imaging microscopy by DJS Cardiac measurements were made using ImageJ (image processing and analysis in Java, http://rsbweb.nih.gov/ij/ (NIH)). Full details are provided in Supplementary information.

Histopathology
Haematoxylin and eosin-stained sections of mammary, endometrial and prostate tumours were analysed blinded to genotype by two experienced histopathologists (BRP and SM). Grading of neoplastic change was made according to published criteria (see Supplementary Information).

miRNA analysis of embryos
RNA was extracted from embryos at E9.5 and hybridised to Illumina mouse microRNA assay pool of 380 mouse microRNAs from Sanger miRBase v9.1 (http://www.mirbase.org/) as described in Supplementary Information (see also http://www.ebi.ac.uk/arrayexpress/experiments/E-MTAB-873).

Cell culture
MCF7 cells were grown in Dulbecco's modified Eagle's medium supplemented with 10% foetal calf serum, 1% glutamine, penicillin and streptomycin in a humidified atmosphere with 5% CO_2 concentration. Stable expression of shRNAs targeting PTEN or a scrambled control sequence in MCF7 cells was achieved by standard retroviral methods as using the P-SuperRetro Puro vector (Oligoengine Seattle, WA, USA), and Phoenix packaging cells (Gentaur Europe, Kamenhout, Belgium, described fully in Supplementary Information). Experiments were performed in serum free Ham's/Dulbecco's modified Eagle's medium 1:1 medium, using recombinant human IGF2 (GroPep, Adeleide, Australia).

Human microarray analysis
Human data sets were downloaded from GEO (Gene Expression Omnibus) and analysed using *R* (http://cran.r-project.org/) as described in Supplementary Information (FMB).

Statistical analysis
Data were compiled in Excel and analysed using GraphPad Prism 5.0 (Graphpad Software Inc, La Jolla, CA, USA). Comparisons between genotypes were made by one-way analysis of variance with Tukey's post-test to adjust for multiple comparisons, with the exception of tumours, which were analysed by non-parametric Kruskal-Wallis test with Dunn's post-test to adjust for multiple comparisons. Comparisons of proportions were made by the χ-square test, or Fisher's exact test when numbers in groups were <5. Survival curves/tumour-free curves were plotted according to the method of Kaplan-Meier with comparison between groups made by the log-rank test. Statistical methods used for analysis of human microarray data are provided in Supplementary Information.

Conflict of interest

The authors declare no conflict of interest.

Acknowledgements

Igf2 knockout mice were a kind gift from Argiris Efstratiadis, *H19*/ICR knockout mice from Shirley Tilghman and *Pten* knockout mice from Ramon Parsons. PTEN shRNA sequences were generously provided by Nick Leslie. We also thank Richard Stillion (histology), Miguel Constancia, Ionel Sandovici, Elisabeth Robertson, Yoichi Sekita and Shuomo Bhattacharya for their helpful discussions. This work was funded by a Cancer Research UK (CRUK) Clinical Research Training Fellowship (DC) and CRUK Programme Grant C429 (ABH).

References

Alimonti A, Carracedo A, Clohessy JG, Trotman LC, Nardella C, Egia A *et al*. (2010). Subtle variations in Pten dose determine cancer susceptibility. *Nat Genet: United States* **42**: 454–458.

Bartolomei MS, Zemel S, Tilghman SM. (1991). Parental imprinting of the mouse H19 gene. *Nature* **351**: 153–155.

Bates P, Fisher R, Ward A, Richardson L, Hill DJ, Graham CF. (1995). Mammary cancer in transgenic mice expressing insulin-like growth factor II (IGF-II). *Br J Cancer* **72**: 1189–1193.

Bayascas JR, Leslie NR, Parsons R, Fleming S, Alessi DR. (2005). Hypomorphic mutation of PDK1 suppresses tumorigenesis in PTEN(+/-) mice. *Current Biology: CB* **15**: 1839–1846.

Bell AC, Felsenfeld G. (2000). Methylation of a CTCF-dependent boundary controls imprinted expression of the Igf2 gene. *Nature* **405**: 482–485.

Burns JL, Hassan AB. (2001). Cell survival and proliferation are modified by insulin-like growth factor 2 between days 9 and 10 of mouse gestation. *Development* **128**: 3819–3830.

Camps C, Buffa FM, Colella S, Moore J, Sotiriou C, Sheldon H *et al*. (2008). hsa-miR-210 Is induced by hypoxia and is an independent prognostic factor in breast cancer. *Clin Cancer Res: United States* **14**: 1340–1348.

Carracedo A, Pandolfi PP. (2008). The PTEN-PI3K pathway: of feedbacks and cross-talks. *Oncogene* **27**: 5527–5541.

Carter AM, Nygard K, Mazzuca DM, Han VK. (2006). The expression of insulin-like growth factor and insulin-like growth factor binding protein mRNAs in mouse placenta. *Placenta* **27**: 278–290.

Chen ML, Xu PZ, Peng XD, Chen WS, Guzman G, Yang X *et al*. (2006). The deficiency of Akt1 is sufficient to suppress tumor development in Pten+/− mice. *Genes Dev* **20**: 1569–1574.

Christofori G, Naik P, Hanahan D. (1994). A second signal supplied by insulin-like growth factor II in oncogene-induced tumorigenesis. *Nature* **369**: 414–418.

Coan PM, Conroy N, Burton GJ, Ferguson-Smith AC. (2006). Origin and characteristics of glycogen cells in the developing murine placenta. *Dev Dyn* **235**: 3280–3294.

Corcoran RB, Bachar Raveh T, Barakat MT, Lee EY, Scott MP. (2008). Insulin-like growth factor 2 is required for progression to

advanced medulloblastoma in patched1 heterozygous mice. *Cancer Res* **68**: 8788–8795.
Crackower MA. (2002). Regulation of myocardial contractility and cell size by distinct PI3K-PTEN signaling pathways. *Cell* **110**: 737–749.
Cui H, Onyango P, Brandenburg S, Wu Y, Hsieh CL, Feinberg AP. (2002). Loss of imprinting in colorectal cancer linked to hypomethylation of H19 and IGF2. *Cancer Res* **62**: 6442–6446.
Cully M, Elia A, Ong SH, Stambolic V, Pawson T, Tsao MS *et al*. (2004). grb2 heterozygosity rescues embryonic lethality but not tumorigenesis in pten+/- mice. *Proc Natl Acad Sci USA* **101**: 15358–15363.
DeChiara TM, Efstratiadis A, Robertson EJ. (1990). A growth-deficiency phenotype in heterozygous mice carrying an insulin-like growth factor II gene disrupted by targeting. *Nature* **345**: 78–80.
DeChiara TM, Robertson EJ, Efstratiadis A. (1991). Parental imprinting of the mouse insulin-like growth factor II gene. *Cell* **64**: 849–859.
Di Cristofano A, De Acetis M, Koff A, Cordon-Cardo C, Pandolfi PP. (2001). Pten and p27KIP1 cooperate in prostate cancer tumor suppression in the mouse. *Nat Genet* **27**: 222–224.
Di Cristofano A, Pesce B, Cordon-Cardo C, Pandolfi PP. (1998). Pten is essential for embryonic development and tumour suppression. *Nat Genet* **19**: 348–355.
Esquiliano DR, Guo W, Liang L, Dikkes P, Lopez MF. (2009). Placental glycogen stores are increased in mice with H19 null mutations but not in those with insulin or IGF type 1 receptor mutations. *Placenta* **30**: 693–699.
Finak G, Bertos N, Pepin F, Sadekova S, Souleimanova M, Zhao H *et al*. (2008). Stromal gene expression predicts clinical outcome in breast cancer. *Nat Med* **14**: 518–527.
Foulstone E, Prince S, Zaccheo O, Burns JL, Harper J, Jacobs C *et al*. (2005). Insulin-like growth factor ligands, receptors, and binding proteins in cancer. *J Pathol* **205**: 145–153.
Frank D, Fortino W, Clark L, Musalo R, Wang W, Saxena A *et al*. (2002). Placental overgrowth in mice lacking the imprinted gene Ipl. *Proc Natl Acad Sci USA* **99**: 7490–7495.
Gabory A, Ripoche MA, Le Digarcher A, Watrin F, Ziyyat A, Forne T *et al*. (2009). H19 acts as a transregulator of the imprinted gene network controlling growth in mice. *Development* **136**: 3413–3421.
Guertin DA, Stevens DM, Saitoh M, Kinkel S, Crosby K, Sheen J-H *et al*. (2009). mTOR complex 2 is required for the development of prostate cancer induced by Pten loss in mice. *Cancer Cell* **15**: 148–159.
Harper J, Burns JL, Foulstone EJ, Pignatelli M, Zaina S, Hassan AB. (2006). Soluble IGF2 receptor rescues Apc(Min/+) intestinal adenoma progression induced by Igf2 loss of imprinting. *Cancer Res* **66**: 1940–1948.
Hassan AB, Howell JA. (2000). Insulin-like growth factor II supply modifies growth of intestinal adenoma in Apc(Min/+) mice. *Cancer Res* **60**: 1070–1076.
Lackey J, Barnett J, Davidson L, Batty IH, Leslie NR, Downes CP. (2007). Loss of PTEN selectively desensitizes upstream IGF1 and insulin signaling. *Oncogene* **26**: 7132–7142.
Leighton PA, Ingram RS, Eggenschwiler J, Efstratiadis A, Tilghman SM. (1995). Disruption of imprinting caused by deletion of the H19 gene region in mice. *Nature* **375**: 34–39.
Li P, Cavallero S, Gu Y, Chen TH, Hughes J, Hassan AB *et al*. (2011). IGF signaling directs ventricular cardiomyocyte proliferation during embryonic heart development. *Development* **138**: 1795–1805.
Liu YF, Paz K, Herschkovitz A, Alt A, Tennenbaum T, Sampson SR *et al*. (2001). Insulin stimulates PKCzeta -mediated phosphorylation of insulin receptor substrate-1 (IRS-1). A self-attenuated mechanism to negatively regulate the function of IRS proteins. *J Biol Chem* **276**: 14459–14465.
Lopez MF, Dikkes P, Zurakowski D, Villa-Komaroff L. (1996). Insulin-like growth factor II affects the appearance and glycogen content of glycogen cells in the murine placenta. *Endocrinology* **137**: 2100–2108.
Ma L, Teruya-Feldstein J, Behrendt N, Chen Z, Noda T, Hino O *et al*. (2005). Genetic analysis of Pten and Tsc2 functional interactions in the mouse reveals asymmetrical haploinsufficiency in tumor suppression. *Genes Dev* **19**: 1779–1786.
Manning BD. (2005). Feedback inhibition of Akt signaling limits the growth of tumors lacking Tsc2. *Genes Dev* **19**: 1773–1778.
Moorehead RA, Hojilla CV, De Belle I, Wood GA, Fata JE, Adamson ED *et al*. (2003). Insulin-like growth factor-II regulates PTEN expression in the mammary gland. *J Biol Chem* **278**: 50422–50427.
Perks CM, Vernon EG, Rosendahl AH, Tonge D, Holly JM. (2007). IGF-II and IGFBP-2 differentially regulate PTEN in human breast cancer cells. *Oncogene* **26**: 5966–5972.
Podsypanina K, Ellenson LH, Nemes A, Gu J, Tamura M, Yamada KM *et al*. (1999). Mutation of Pten/Mmac1 in mice causes neoplasia in multiple organ systems. *Proc Natl Acad Sci USA* **96**: 1563–1568.
Ravichandran LV, Esposito DL, Chen J, Quon MJ. (2001). Protein kinase C-zeta phosphorylates insulin receptor substrate-1 and impairs its ability to activate phosphatidylinositol 3-kinase in response to insulin. *J Biol Chem* **276**: 3543–3549.
Reardon W, Zhou XP, Eng CC. (2001). A novel germline mutation of the PTEN gene in a patient with macrocephaly, ventricular dilatation, and features of VATER association. *J Med Genet* **38**: 820–823.
Sakatani T, Kaneda A, Iacobuzio-Donahue CA, Carter MG, de Boom Witzel S, Okano H *et al*. (2005). Loss of imprinting of Igf2 alters intestinal maturation and tumorigenesis in mice. *Science* **307**: 1976–1978.
Singer C, Rasmussen A, Smith HS, Lippman ME, Lynch HT, Cullen KJ. (1995). Malignant breast epithelium selects for insulin-like growth factor II expression in breast stroma: evidence for paracrine function. *Cancer Res* **55**: 2448–2454.
Soroceanu L, Kharbanda S, Chen R, Soriano RH, Aldape K, Misra A *et al*. (2007). Identification of IGF2 signaling through phosphoinositide-3-kinase regulatory subunit 3 as a growth-promoting axis in glioblastoma. *Proc Natl Acad Sci USA* **104**: 3466–3471.
Trimboli AJ, Cantemir-Stone CZ, Li F, Wallace JA, Merchant A, Creasap N *et al*. (2009). Pten in stromal fibroblasts suppresses mammary epithelial tumours. *Nature* **461**: 1084–1091.
Trotman LC, Alimonti A, Scaglioni PP, Koutcher JA, Cordon-Cardo C, Pandolfi PP. (2006). Identification of a tumour suppressor network opposing nuclear Akt function. *Nature* **441**: 523–527.
Tsang WP, Ng EK, Ng SS, Jin H, Yu J, Sung JJ *et al*. (2010). Oncofetal H19-derived miR-675 regulates tumor suppressor RB in human colorectal cancer. *Carcinogenesis* **31**: 350–358.
van Roozendaal CE, Gillis AJ, Klijn JG, van Ooijen B, Claassen CJ, Eggermont AM *et al*. (1998). Loss of imprinting of IGF2 and not H19 in breast cancer, adjacent normal tissue and derived fibroblast cultures. *FEBS Lett* **437**: 107–111.
Veronese A, Lupini L, Consiglio J, Visone R, Ferracin M, Fornari F *et al*. (2010). Oncogenic role of miR-483-3p at the IGF2/483 locus. *Cancer Res* **70**: 3140–3149.
Wang H, Karikomi M, Naidu S, Rajmohan R, Caserta E, Chen HZ *et al*. (2010). Allele-specific tumor spectrum in pten knockin mice. *Proc Natl Acad Sci USA: United States* **107**: 5142–5147.
Yang ZZ, Tschopp O, Hemmings-Mieszczak M, Feng J, Brodbeck D, Perentes E *et al*. (2003). Protein kinase B alpha/Akt1 regulates placental development and fetal growth. *J Biol Chem* **278**: 32124–32131.
Yoshimizu T, Miroglio A, Ripoche MA, Gabory A, Vernucci M, Riccio A *et al*. (2008). The H19 locus acts *in vivo* as a tumor suppressor. *Proc Natl Acad Sci USA* **105**: 12417–12422.